Hot-electron relaxations and hot phonons in GaAs studied by subpicosecond Raman scattering

Dai-sik Kim and Peter Y. Yu
Department of Physics, University of California, Berkeley, California 94720
and Materials and Chemical Sciences Division, Lawrence Berkeley Laboratory,
1 Cyclotron Road, Berkeley, California 94720
(Received 11 June 1990; revised manuscript received 13 September 1990)

We have utilized subpicosecond laser pulses to excite and probe hot electrons and nonequilibrium longitudinal-optical (LO) phonons in bulk GaAs by Raman scattering. We find that the photoexcited hot electrons cool at a rate much faster than predicted by *intra*valley scattering of LO phonons via the Frölich interaction. On the other hand, this fast cooling rate can be accounted for satisfactorily by *inter*valley scattering. As a result of this very rapid cooling, the temperature of the hot LO phonons generated by the hot electrons temporarily overshoots the electron temperature. From the electron cooling curve and the dependence of the hot-phonon temperature on the excited-electron density, we determined the deformation potential for scattering between the Γ and L conduction-band valleys in GaAs.

I. INTRODUCTION

It has been known for many years that energetic electrons in GaAs relax predominantly via electron-phonon interactions.[1,2] Of the many types of electron-phonon interactions possible in GaAs, the interaction between electrons and the zone-center longitudinal-optical (LO) phonons and the zone-edge optical phonons are known to occur in subpicosecond time scale.[2] Recently, with the appearance of femtosecond dye lasers, it becomes possible to study these fast interactions in real time. So far there have been many reports on the study of fast relaxation of hot electrons in GaAs excited by femtosecond lasers using optical techniques such as absorption[3–5] and emission.[6] Comparatively, there are very few studies of hot-electron relaxation using Raman scattering.[7,8] Raman scattering has the advantages of being an instantaneous process and being able to probe both electrons and phonons in the same experiment. However, Raman scattering also has the disadvantages that the Raman signals due to photoexcited hot electrons and phonons are very small.

In this paper we present the results of a study of hot-electron relaxation using subpicosecond Raman scattering. We overcome the difficulty of weak Raman signals by using the same subpicosecond laser beam to excite and probe the hot electrons and phonons. We have shown elsewhere[9,10] by using model calculations how the cooling rate of hot electrons can be determined in such a single-beam Raman experiment by varying the laser pulse width. In this paper we applied the single-beam technique to measure the dependence of electron temperature and phonon population on photoexcited electron densities. We find that at electron densities higher than 10^{18} cm^{-3} the "effective phonon temperature" overshoots that of the electrons (a phenomenon we have labeled phonon temperature overshoot).[11] By comparing our results with simple model calculations based on a realistic band structure of GaAs we have been able to explain our results and to determine the electron-phonon scattering times for both *intra*valley and *inter*valley scatterings. Futhermore, we have clarified the role of hot phonons in the relaxation of hot electrons in GaAs.

The organization of this paper is as follows. In Sec. II we present the background theories and models for understanding the relaxation of hot electrons excited by femtosecond laser pulses. We will start with a commonly used model in which the conduction band is assumed to have only one minimum at the Brillouin-zone center. Since the photoexcited electrons in GaAs often have sufficient energy to scatter into the higher conduction-band valleys, we also consider a multivalley conduction-band model. The effects of the laser pulse width are then included in the theory. Following the theoretical considerations, we describe the details of our experimental setup and sample configurations. The technique of using a single subpicosecond laser beam to perform Raman scattering from photoexcited hot electrons and hot phonons will be presented. The kind of information one can extract using this technique is discussed. The electron and phonon temperatures measured with this technique as a function of excited carrier densities and of laser pulse length are presented. Finally, by comparing the experimental results with the predictions of both the one-valley model and the multivalley model, we show that the experimental results cannot be explained by the one-valley model, but are in good agreement with the predictions of the multivalley model.

II. MODEL CALCULATIONS

In this section we present simple model calculations of the cooling curves of photoexcited hot electrons in bulk GaAs and the corresponding increase in longitudinal-optical phonon population caused by the relaxation of hot electrons. We will consider two band models which have been commonly used in the literature. Both models are based on the schematic band structure of GaAs

shown in Fig. 1. In the first model the band structure of GaAs is approximated by two spherical bands only (one conduction and one valence band). In spite of its simplicity this model has been used extensively in the literature.[12,13] For the rest of this paper this model will be referred to as the two-band one-valley model (or abbreviated as the one-valley model). In the second model a realistic conduction band with minima at the center, L points, and X points of the Brillouin zone is used while the valence band is still assumed to be spherical. The second model will be referred to as the two-band multivalley model (abbreviated as the multivalley model).

A. One-valley model

In this model we will consider only the conduction band and heavy-hole bands in GaAs and assume that both bands are isotropic. The heavy-hole band dispersion is assumed to be parabolic with effective mass m_h while the conduction-band dispersion is assumed to be nonparabolic:

$$\hbar^2 k^2/2m^* = E_k + \alpha E_k^2 + \beta E_k^3 , \quad (1)$$

where m^* is the conduction-band effective mass and E_k is the energy of electron with wave vector k. The values of m_h, the conduction-band parameters α and β, and other parameters to be used in our calculations are given in Table I. In this model the presence of higher conduction minima in GaAs is neglected. This simple model has been used widely to interpret experimental results on the cooling of hot carriers in GaAS (Ref. 12) because it is generally thought that intervalley scatterings are important for depleting electron population in the Γ valley but not for cooling the Γ-valley electrons.

We will assume that hot-electron–hole pairs are excited by an infinitesimally short pulse with photon energies of about 0.5 eV above the band gap of GaAs. This excess energy in the photons are translated into kinetic energies of the excited electrons and hole. In general, the distribution functions of the excited electrons and holes are nonthermal. Monte Carlo simulation techniques are necessary to calculate how these nonthermal distributions attain equilibrium.[14] Unfortunately, such calculations are very complex and often require the use of fast supercomputers. Most of these Monte Carlo calculations have been performed for times longer than a picosecond after excitation by a short laser pulse and so cannot be compared with our subpicosecond results. In the absence of available theoretical calculation for direct comparison with our results we have interpreted our results with highly simplified albeit realistic models which are more amenable to analytical calculations. To make such calculation possible without using Monte Carlo simulation we have to assume that the electrons and holes attain separate quasiequilibrium *instantaneously*. This assumption is justified for photoexcited carriers with concentration higher than 10^{18} cm^{-3}, where it has been found that electrons reach thermal equilibrium in 100 fs and less.[5,6,15,16] Since the electrons have much smaller masses than the heavy holes, most of the excess energy in the photon is translated into kinetic energy for the electrons. We will assume, therefore, that the heavy holes have essentially the temperature of the lattice (either 77 or 300 K) while the electron temperature T_e will be given by

$$T_e = 2(\hbar\omega - E_g)/(3k_B) \quad (2)$$

where $\hbar\omega$ is the photon energy, E_g is the band gap of GaAs, and k_B is Boltzmann's constant. For $\hbar\omega = 2.0$ eV

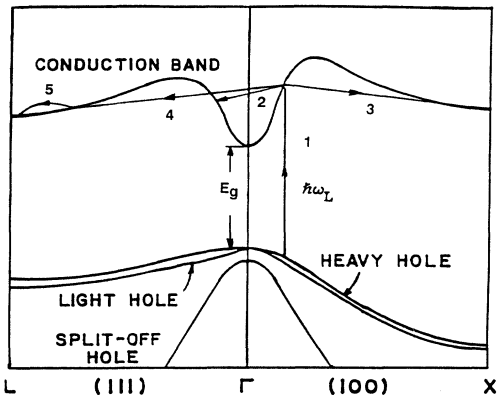

FIG. 1. Schematic band structure of the lowest conduction band and the highest valence band of GaAs. The arrow labeled 1 represents optical excitation of electrons and holes. Arrow 2 represents *intra*valley scattering of electrons by LO phonons while arrows 3–5 represent *inter*valley scattering processes. Both types of scattering processes contribute to the relaxation of hot electrons in subpicosecond regime.

TABLE I. Relevant material parameters of GaAs.

Band Gap at 300 K	1.424 eV
Conduction-band parameters:	
α	0.577 eV^{-1}
β	0.047 eV^{-2}
Energy separation between Γ and X minima	0.47 eV
Energy separation between Γ and L minima	0.29 eV
Γ-valley effective mass	$0.067m_e$
L-valley density-of-states mass	$0.22m_e$
X-valley density-of-states mass	$0.407m_e$
$D_{\Gamma-X}$	10×10^8 eV/cm
$(1/\epsilon_\infty)-(1/\epsilon_0)$	0.017

used in our experiment, T_e is of the order of 3000 K. In this paper we are interested mainly in the cooling of this hot-electron gas *within* 1 ps *after excitation.* In such a short time scale the dominant cooling mechanism is the emission of LO phonons via the Fröhlich interaction (represented by arrow 2 in Fig. 1) because the other mechanisms such as emission of acoustic phonons and transverse-optical (TO) phonons are too slow to be significant.[2] Electron-hole (*e-h*) scattering can cool the hot electrons also since the holes are much colder than the electrons. Electron-hole scattering involves many-body interactions which depend in a complicated manner on density. Using the ensemble Monte Carlo method, Osman and Ferry[17] have calculated the energy loss rate of hot electrons due to *e-h* scattering. For electron and hole densities both equal to 10^{18} cm^{-3} they found an energy loss rate of 60 meV/ps, which is about three times smaller than for electron–LO-phonon scattering so we will neglect *e-h* scattering unless the experimental results suggest otherwise. Finally, we will neglect diffusion of the photoexcited carriers because in our sample the carriers are confined inside the GaAs layer by AlAs layers on both sides. Lateral diffusion of carriers within the GaAs layer is negligible within 1 ps.

With the above assumptions we can calculate the rate of generation of LO phonons by the relaxation of hot electrons having a distribution function $f(E_{\mathrm{k}})$. The rate equation for the LO-phonon population N_{q} can be shown to be given by[18]

$$\frac{\partial N_q}{\partial t}=\frac{1}{q^3}[-N_q A_q+(N_q+1)B_q] , \tag{3}$$

where q is the LO-phonon wave vector. The coefficients A_{q} and B_{q} describe, respectively, the absorption and emission of LO phonons by the hot electrons. In Eq. (3) we have neglected the decay of the LO phonons because the LO-phonon lifetime in GaAs is about 4–7 ps,[13] while we will be interested in the solution of Eq. (3) within 1 ps. Using the usual expression for the Fröhlich interaction and assuming parabolic conduction band, A_{q} and B_{q} can be shown to be given by[18]

$$A_q=\frac{2m^{*2}\omega_{\mathrm{LO}}e^2}{\hbar^4}\left[\frac{1}{\epsilon_\infty}-\frac{1}{\epsilon_0}\right] \times\int_{E_q^1}^{\infty} f(E_K)[1-f(E_K-E_{\mathrm{LO}})]dE_K , \tag{4}$$

$$B_q=\frac{2m^{*2}\omega_{\mathrm{LO}}e^2}{\hbar^4}\left[\frac{1}{\epsilon_\infty}-\frac{1}{\epsilon_0}\right] \times\int_{E_q^2}^{\infty} f(E_K)[1-f(E_K+E_{\mathrm{LO}})]dE_K , \tag{5}$$

where ω_{LO} and E_{LO} are, respectively, the LO-phonon frequency and energy, and ϵ_0 and ϵ_∞ are, respectively, the low-frequency and high-frequency dielectric constants of GaAs. The lower energy limits of integration in Eqs. (4) and (5) are defined as

$$E_q^1=\frac{(E_q-E_{\mathrm{LO}})^2}{4E_q} , \tag{6}$$

$$E_q^2=\frac{(E_q+E_{\mathrm{LO}})^2}{4E_q} , \tag{7}$$

where $E_q=\hbar^2q^2/2m^*$, and E_q^1 and E_q^2 are, respectively, the minimum electron energies for absorption and emission of a LO phonon with wave vector q.

We note that in Eq. (3) the factor q^{-3} results from a q^{-2} dependence in the Fröhlich matrix element. Since the Fröhlich interaction involves Coulomb interaction between charges and the macroscopic electric field of the LO phonon, at high electron densities we expect this interaction to be reduced due to screening.[17,19] Such screening effects have been proposed to explain the decrease in the hot-electron cooling rate at high electron densities.[12] The calculation of this screening is a complicated problem in our case since both electrons and holes are excited optically. The problem will be even more complicated if we assume that the electrons are distributed in several valleys as we will do in the multivalley model. Again in the spirit of simplicity, we will assume that all the electrons are in the Γ valley and the effect of screening can be included by rewriting the Fröhlich matrix element $|M_{\mathrm{q}}|^2$ as

$$|M_{\mathrm{q}}|^2\propto(q^2+k_s^2)^{-1} , \tag{8}$$

where k_s denotes the screening vector.[20] As an illustration, we will mainly be interested in LO phonons with $q=7.5\times10^5$ cm^{-1}, while k_s is about 4×10^5 cm^{-1} for an electron gas of density 10^{18} cm^{-3} and temperature 3000 K. Thus the effect of screening is to reduce the LO-phonon emission rate by about 30%. As we will see later, the actual screening effect is even smaller than that given by this estimate because some of the hot electrons are located in the higher conduction-band valleys where they have larger masses and correspondingly smaller screening vectors.

Once the rate of emission of LO phonons by the hot electrons has been calculated from Eq. (3), the rate of decrease of the average electron energy $\langle E\rangle$ can be computed with this expression:

$$\frac{\partial\langle E\rangle}{\partial t}=-\frac{E_{\mathrm{LO}}}{n_e}\int\frac{\partial N_q}{\partial t}\rho_q dq , \tag{9}$$

where n_e is the electron density and ρ_q is the LO-phonon density of states in GaAs. The latter quantity is known from the experimental phonon dispersion curves. As an illustration of the predictions of Eqs. (3) and (9) we have computed T_e and N_q for a hot-electron gas with $n_e=3\times10^{18}$ cm^{-3} and initial temperature 3000 K, both representing conditions realized in our experiment. The parameters used in the calculation can be found in Table I. The time to emit one LO phonon deduced from these parameters is about 200 fs. In displaying our results we will use an effective phonon temperature T_q instead of N_q with the two quantities related by

$$N_q=[\exp(E_{\mathrm{LO}}/k_bT_q)-1]^{-1} . \tag{10}$$

Our reason for using a phonon temperature rather than the phonon population is that temperature is a more in-

tuitive parameter for discussing energy exchange between electrons and phonons. For example, we expect electrons to cool by emission of LO phonons when $T_e > T_q$ and to heat up by absorbing phonon when $T_q > T_e$. We should point out that we have no information as to whether the phonons are in quasithermal equilibrium and have, therefore, a well-defined temperature. A better understanding of the phonon-phonon interaction is necessary to answer this question.

The calculated time dependence of T_e and T_q is shown in Fig. 2 for three different values of q. Several features of these results should be noted. First the electron temperature remains quite high even after 1 ps. This is a result of the relatively slow cooling rate via LO-phonon emission. The temperature of the small-q phonons rises faster than the temperature of phonons with larger q. The is due to the q^{-3} dependence in the phonon generation rate. Finally, we notice that, for $q = 8\times10^5$ cm^{-1}, T_q actually overshoots T_e slightly after about 500 fs. This occurs as a result of continued cooling of electrons by emission of larger-q LO phonons even though the smaller-q LO phonons have already temperatures slightly higher than T_e. This very small temperature overshoot means that the smaller-q phonons are no longer effective in cooling the hot electrons after T_e has dropped below about 2500 K. The presence of hot phonons cause the electron cooling rate (given by the slope of the cooling curve) to decrease slowly as the electron temperature drops. This decrease of the electron cooling rate at high electron densities have been referred to as the "hot-phonon effect."[14,21–24] The present calculation differs from the previous work on the hot-phonon effect in that previous calculations are for longer time delays. We note from our calculation that the smaller-q hot LO phonons are responsible for the decrease in phonon cooling rate at time less than 1 ps whereas the larger-q hot phonons are effective after several picoseconds.

B. Multivalley model

It has been known for a long time that electrons with sufficient energy above the Γ conduction-band minimum can scatter into the higher conduction-band valleys at the L and X points of the Brillouin zone with emission of a zone-edge phonon.[2,18] The time to scatter to the X valley is even shorter than the LO-phonon scattering time. The time to scatter into the L valleys is known with less certainty. Estimates of this time varies from about 50 to 1 ps.[25] Thus intervalley scattering (IVS) can be a very efficient channel for cooling the hot electrons in the Γ valley. For this is to be true, it is necessary to keep in mind that IVS only temporarily removes the high-energy electrons in the Γ valley. The electrons which scatter to the L and X minima will eventually return to the Γ valley. However, this return process takes typically several picoseconds because of the smaller density of final states in the Γ valley.[6] Thus, within 1 ps we can regard the high-energy electrons as being completely removed by IVS. Since the L and X conduction-band minima are about 0.3 and 0.46 eV above the Γ minimum, IVS is important only when the electron temperature is high. Otherwise there will be very few electrons with such energy to undergo IVS. Recently Rota and Lugli[14] point out that the electrons scattered into the higher conduction-band valleys by IVS have lower energy than the electrons in the Γ valley and can therefore contribute to the cooling of hot electrons in the Γ valley. This electron-electron scattering mechanism is strongly dependent on electron density as in the case of electron-hole scattering. For total electron density of 10^{18} cm^{-3}, Rota and Lugli showed that the electron-electron scattering contribution to the hot-electron cooling rate becomes comparable to the electron–LO-phonon contribution. Thus the electron-electron scattering contribution to cooling of hot electrons in the Γ valley is still negligible when compared to IVS. This conclusion is also consistent with our experimental observation that the electron temperature increases slightly with electron density rather than decreasing with density as would be expected if electron-electron scattering becomes the dominant cooling mechanism at high electron densities.

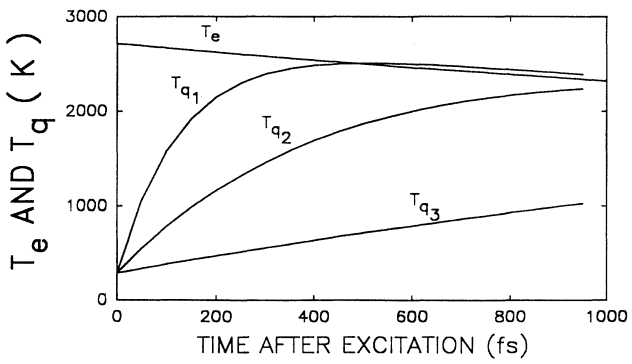

FIG. 2. Theoretical cooling curve of hot electron and hot phonons (with wave vector $q_1, q_2, q_3 = 8$, 15, and 30×15^5 cm^{-1}, respectively) calculated excited by laser pulses of 0 fs FWHM calculated with the one-valley model.

To calculate the time dependence of T_e and T_q including IVS, we introduce one additional rate equation for the electron population in the Γ valley (N_Γ) and modify Eq. (9) for the cooling of the hot electrons. The rate of decrease in N_Γ due to IVS is given by

$$\frac{\partial N_\Gamma}{\partial t} = \int \left[\frac{\partial f}{\partial t}\right]_{\Gamma-L,X} \rho_\Gamma dE_\Gamma \ , \tag{11}$$

where $(\partial f/\partial t)_{\Gamma-L,X}$ represents the rate of decrease in the electron occupation number in the Γ valley due to IVS to the L and X conduction-band valleys, and ρ_Γ and E_Γ are, respectively, the density of states and energy of electrons in the Γ valley. $(\partial f/\partial t)_{\Gamma-L,X}$ is the sum of the individual rates $(\partial f/\partial t)_{\Gamma-L}$ and $(\partial f/\partial t)_{\Gamma-X}$, which can be expressed in terms of the IVS deformation potentials $D_{\Gamma-L}$ and $D_{\Gamma-X}$ and the effective masses of the L and X valleys. Expressions for $(\partial f/\partial t)_{\Gamma-L}$ and $(\partial f/\partial t)_{\Gamma-X}$ can be found, for example, in Ref. 18. It should be noted that both rates depend on E_Γ. For simplicity we will make the same assumption as in Ref. 18 that all the zone-edge phonons [except for the transverse acoustic

(TA) (L) phonon] have the same frequency ω_{ZB} with $\hbar\omega_{ZB}=29.6$ meV. The rate of decrease in the average energy (and hence temperature) of electrons in the Γ valley is now given by

$$\frac{\partial(N_\Gamma\langle E_\Gamma\rangle)}{\partial t}=\int\left[\frac{\partial f}{\partial t}\right]_{\Gamma-L,X}\rho_\Gamma E_\Gamma dE_\Gamma - \hbar\omega_{\mathrm{LO}}\int\frac{\partial N_q}{\partial t}\rho_q dq \ . \tag{12}$$

By repeating the calculation of the time dependence of T_e and T_q using Eqs. (3), (11), and (12) we obtained the cooling curves in Fig. 3. The value of **q** in this calculation is 7.5×10^5 cm^{-1}, while the value of $D_{\Gamma-L}$ is chosen to be 7×10^8 eV/cm. The total excited electron density is still 3×10^{18} cm^{-3}, although it should be noted that the electron density inside the Γ valley, N_Γ, is now less than the total electron density because of IVS. It is clear that the behaviors of T_e and T_q are quite different from those in Fig. 2. As a result of IVS, T_e now decreases to about 1500 K in 100 fs. This corresponds to a cooling rate of about 2.6 eV/ps or more than one order of magnitude faster than the cooling rate via LO-phonon emission. Within 100 fs about 50% of the electrons in the Γ valley have transferred to the X and L valleys.[26] Because we have assumed that the electrons thermalize instantaneously, the electron temperature drops rapidly as the high-energy electrons are removed. *This shows that for time shorter than 1 ps, the predominant cooling mechanism of high-energy electrons in GaAs is due to IVS.* During the same time interval the increase in T_q is not changed significantly from that shown in Fig. 2. However, instead of continuing to increase to over 2000 K, T_q stops increasing as the phonon temperature crosses the electron temperature and then overshoots T_e by several hundred degrees. From Fig. 3 we note that it takes the LO phonon and Γ electrons about 1 ps to reach equilibrium because when the electrons have cooled to below 1000 K there are very few high electrons left that can absorb the small momentum LO phonons. By varying the parameters used in our calculation we find that the electron

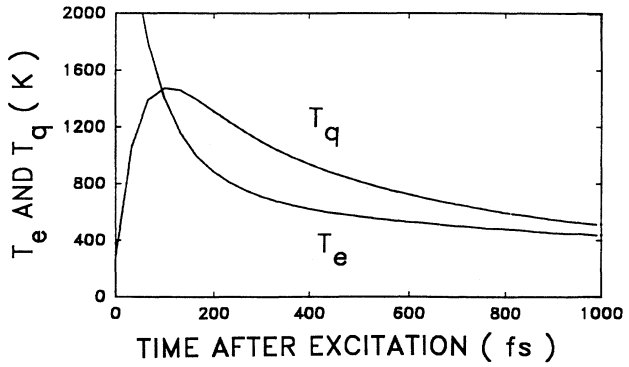

FIG. 3. Theoretical time dependence of T_e and T_q ($q=7.5\times10^5$ cm^{-1}) calculated with the mulitvalley model described in the text. The deformation potential $D_{\Gamma-L}$ is adjusted to 7×10^8 eV/cm.

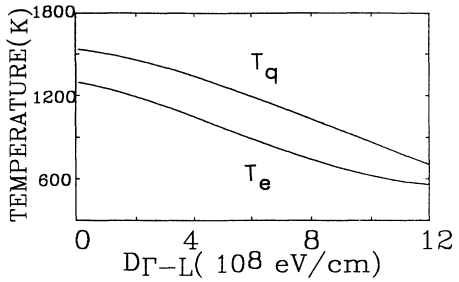

FIG. 4. Calculated T_e and T_q ($q=7.5\times10^5$ cm^{-1}) at 200 fs after excitation by a δ-function laser pulse plotted as a function of $D_{\Gamma-L}$ for $N_e=3\times10^{18}$ cm^{-3}.

and phonon temperatures around 200 fs after excitation are quite sensitive to the value of the deformation potential $D_{\Gamma-L}$. Figure 4 shows the dependence of T_e and T_q on $D_{\Gamma-L}$. We note that T_q overshoots T_e even if we neglect the Γ to L IVS. The effect of IVS from Γ to L is to provide additional cooling of T_e after the electron gas has become too cold to scatter to the X valleys. After about 400 fs the electron cooling rate slows down significantly because the electron temperature has dropped below 700 K so there are not enough hot electrons to scatter to the L valleys. Beyond 500 fs *intra*valley scattering with LO phonons becomes the dominant cooling mechanism.

C. Effect of finite pulse duration

So far we have assumed in our model calculation that the laser pulses are infinitesimally short in duration. In our experiment we will be using laser pulses of approximately sech^2 temporal shape having a full width at half maximum (FWHM) of about 600 fs. The effect of finite pulse width on subpicosecond Raman scattering from photoexcited hot electrons excited and probe by a single laser beam have been reported by us in Ref. 10. We have shown via simulation that, when the laser pulse FWHM is δt, the measured electron temperature is roughly equal to the temperature of electrons, which have been excited by an infinitesimally short pulse and then cooled for a time duration of $0.4\delta t$. In this paper we will consider also the effect of finite pulse duration on the phonon temperature. We will assume that the laser-pulse profile $I(t)$ is given by

$$I(t)=I_0\mathrm{sech}^2(1.76t/\delta t) \ . \tag{13}$$

Equations (11) and (12) are modified to include the continuous excitation of electrons in the Γ valley and heating of the electron gas by this addition of hot electrons:

$$\frac{\partial N_\Gamma}{\partial t}=\int\left[\frac{\partial f}{\partial t}\right]_{\Gamma-L,X}\rho_\Gamma dE_\Gamma+R(t) \ , \tag{14}$$

$$\frac{\partial(N_\Gamma\langle E_\Gamma\rangle)}{\partial t}=\int\left[\frac{\partial f}{\partial t}\right]_{\Gamma-L,X}\rho_\Gamma E_\Gamma dE_\Gamma - \hbar\omega_{\mathrm{LO}}\int\frac{\partial N_q}{\partial t}\rho_q dq+R(t)E(0) \ , \tag{15}$$

where $R(t)$ is the rate of photoexcitation of electrons and holes calculated assuming that the electron and hole densities are uniform within the absorption length. $E(0)$ is the initial kinetic energy of the electron immediately after excitation. By repeating the calculations in Sec. II B we obtain the cooling curves of electrons and LO phonons excited by laser pulses with δt equal to 600 fs as shown in Fig. 5. The center of the laser pulse was taken to be $t=0$. The other parameters are same as in Fig. 3, except that the total excited electron density (n_e) is increased to about 5×10^{18} cm^{-3} so that the maximum electron in the Γ valley (N_Γ) is now equal to 3×10^{18} cm^{-3}. We note that the general trend of T_e and T_q depicted in Figs. 3 and 5 are similar, especially the phonon temperature overshoot of the electron temperature is unchanged. There are, however, differences. The most interesting one is that around $t=0$ the phonon temperature shows a broad maximum while the electron temperature shows a dip and weak maximum. The explanation is simply that the laser pulse peaks at $t=0$ so the addition of a large amount of hot electrons by the laser pulse near $t=0$ slows the cooling of the electrons already present. In Fig. 5 we show also N_Γ, the electron density in the Γ valley, as a function of time. Notice that because of IVS, N_Γ is not simply given by the integral of $R(t)$. If there were no IVS, $N_\Gamma(0)$ will be equal to one-half of the maximum value of N_Γ.

In case of photoexcited hot electrons we have shown that the electron cooling curve can be measured by using a single laser beam to both excite and probe the hot electrons by Raman scattering.[10] The time dependence of the hot-electron temperature can be deduced from the dependence of the electron temperature on *pulse length*.[9,10] This is not possible for phonons. The electron temperature always decreases monotonically in a way independent of the electron density. However, the phonon temperature increases first and then decreases with time. The rate of increase of the phonon temperature depends on the density of hot electrons in the Γ valley. As a result, if we compute the phonon temperature averaged over the laser pulse length, the result depends more on the laser power density than on the pulse length. On the other hand, the time-averaged phonon temperature is close to the maximum phonon temperature since the phonons remain at this temperature over much of the laser pulse as shown in Fig. 5. Thus we can conclude that the effect of using a laser pulse of nonzero width to both excite and probe hot electrons and LO phonons by Raman scattering is that the measured T_e represents the temperature of an electron gas excited by a δ-function pulse after cooling for a duration equal to $0.4\delta t$ while the measured T_q is equal to the maximum phonon temperature.

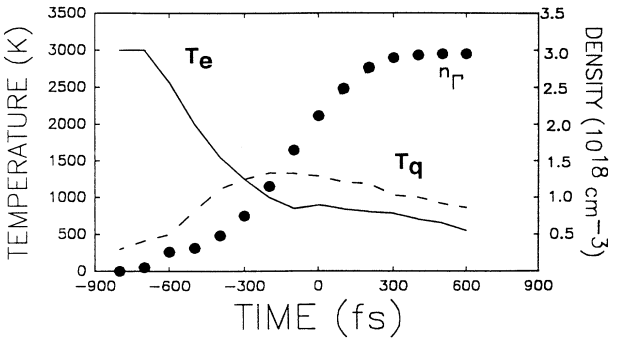

FIG. 5. Theoretical time dependence of T_e, T_q ($q=7.5\times10^5$ cm^{-1}), and n_Γ calculated with the multivalley model described in the text. The laser pulse width is 600 fs FWHM. The deformation potential used for this calculation is 7×10^8 eV/cm.

III. EXPERIMENTAL DETAILS

The setup used in this experiment is shown schematically in Fig. 6. The heart of this setup is the colliding-pulse mode-locked (CPM) dye laser, which is pumped by an Ar ion laser. The typical CPM laser containing four prisms inside the cavity to compensate for group velocity dispersion produces laser pulses with widths of about 100 fs and bandwidths of 150 cm^{-1} using Rhodamine 6G as the lasing dye and 3,3′-diethyloxadicarbocyanine iodide (DODCI) as the saturable absorber.[27,28] This bandwidth is too broad for us to observe the phonons of GaAs by Raman scattering. As a result we have replaced the four prisms with birefringent plates as wavelength selecting elements. The laser pulses from our CPM laser has bandwidths of 30 cm^{-1} and a FWHM of 600 fs. The pulse width can be varied discretely between 200 and 800 fs by changing the concentration of DODCI or the birefringent plates. The repetition rate of our laser pulse is 120 MHz, the photon energy is about 2 eV, and the average power is about 30 mW. One of the two output beams from the CPM laser is sent into an autocorrelator to monitor the laser-pulse shape and stability. The autocorrelator curves can be fitted very well by assuming that the laser pulses have a sech^2 dependence on time.[29] The other beam is sent through a Brewster angle prism to

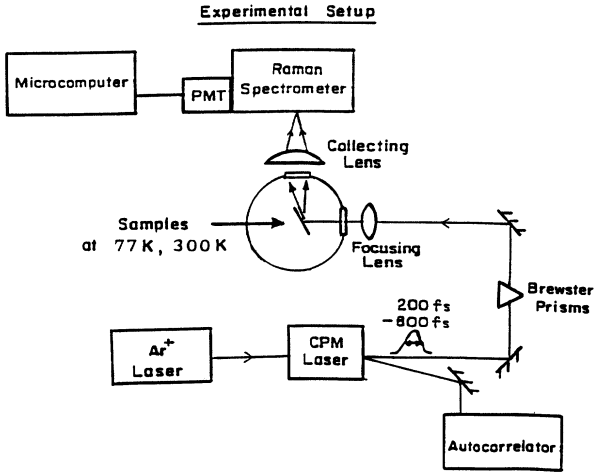

FIG. 6. Schematic diagram of the apparatus for performing one-beam excite-and-probe Raman experiment with the CPM laser.

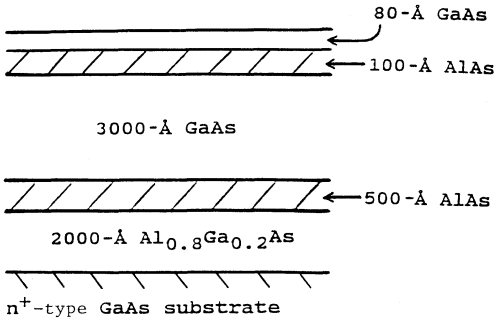

FIG. 7. Structure of the GaAs sample used in our experiments. The 0.3-μm GaAs layer is sandwiched between two AlAs layers to prevent the carriers from diffusing into the substrate.

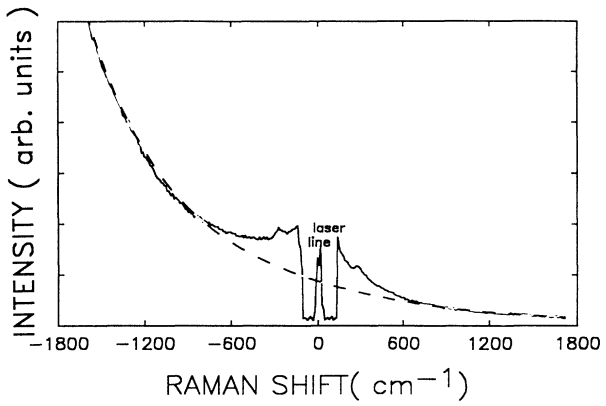

FIG. 8. Typical emission spectrum of GaAs when excited by subpicosecond pulses from the CPM laser superimposed on the hot luminescence background (dashed line).

filter out the dye fluorescence before being focused on the sample. The size of the focal spot on the sample can be estimated from the magnified image of the focal spot viewed through the periscope on the Spex 1403 double monochromator. The laser intensity profile was found to be essentially Gaussian. The maximum density of electrons excited by the laser pulse was varied between 10^{17} and 10^{19} cm^{-3} (at the center of the Gaussian intensity profile) by changing the size of the laser focus between 100 and 10 μm.

Figure 7 shows the structure of the sample which consists of a 3000-Å-thick GaAs sample grown by molecular-beam epitaxy (MBE) on a [001] substrate. The GaAs layer was sandwiched between two AlAs layers to prevent carrier diffusion into the substrate. The top AlAs layer was protected by a thin layer of GaAs to prevent oxidization of AlAs. The incident and backscattered radiations are polarized along the $[1\bar{1}0]$ directions. In this scattering geometry both electronic and LO-phonon Raman scatterings are allowed. We note that the wave vector of the LO phonon probed by our backscattering geometry is determined by the incident photon energy to be 7.5×10^5 cm^{-1}. The scattered photons are detected by a cooled photomultiplier tube and photon counting electrons. It should be noted that the same laser pulses are used to both excite and probe the hot electrons and also the hot phonons generated by the relaxation of the hot electrons.

IV. EXPERIMENTAL RESULTS

A typical emission spectrum obtained at about 77 K by focusing the output of the CPM laser on our GaAs sample is shown in Fig. 8. This scattered spectrum can be decomposed into three parts: (a) a broad background due to luminescence extending all the way to the band gap of GaAs around 1.5 eV; (b) relatively sharp peaks caused by scattering from the LO-plasmon modes on both side of the laser line; and (c) a broader peak centered on the laser line caused by scattering from single-particle excitations (SPE) of the photoexcited electron plasma.

The luminescence spectrum in this small range of energy around 2 eV can be fitted rather well by a single exponential as shown by the dashed line in Fig. 8. An example of the entire time-integrated photoluminescence spectrum of the GaAs sample excited by the CPM laser is shown as the continuous curve in Fig. 9 (this spectrum was taken at 300 K). It is very broad because of the high carrier density excited by the short CPM laser pulses. To fit the luminescence spectra, we assume that the electron gas is highly degenerate and treat the electron temperature T_e and quasi-Fermi energy μ as adjustable parameters. On the other hand, the holes are assumed to thermalize immediately to a Boltzmann distribution with the same temperature as the lattice.[6] With these assumptions the luminescence line shape can be fitted by the following equation:[30]

$$I(E)\propto\sqrt{E-E_g}\,e^{-E_h/k_bT_h}\frac{1}{e^{(E_e-\mu/k_bT_e)}+1}\,, \tag{16}$$

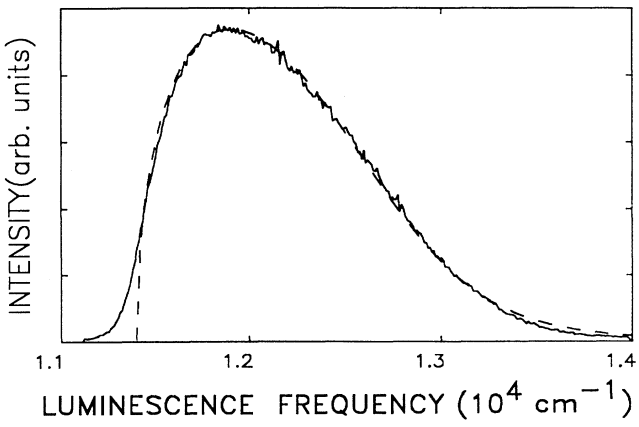

FIG. 9. Time-integrated photoluminescence spectrum of GaAs excited by laser pulses of 600 fs. The pulse energy was 0.2 nJ per pulse and the focal size was about 20 μm. The dashed curve is a fit to the experimental curve with Eq. (16) in the text.

where $\hbar\omega = E_g + E_\Gamma + E_h$, $E_\Gamma / E_h = m_h / m^*$, and E_h is the energy of the heavy hole. We find that the electron temperatures are typically around 500 K as determined from fitting the luminescence spectra (shown as the dashed curve in Fig. 9) when the lattice temperature is 300 K. This suggests a small amount of heating of the lattice by the laser beam within the decay time of the photoexcited electron-hole plasma which is estimated to be of the order of a nanosecond or less. The Fermi energy determined by fitting the luminescence spectrum is $\mu = 155$ meV, corresponding to an electron density of around 5×10^{18} cm^{-3}. This density is quite close to the value of 10^{19} cm^{-3} calculated from the GaAs absorption coefficient, laser energy, and focal spot size. The reason for the luminescence density to be so close to the calculated density of electrons excited by the laser pulse is because the electrons that have scattered into the higher conduction valleys eventually return to the Γ valley. The fact that the time-integrated and calculated electron densities are equal to within a factor of 2 suggests that lateral diffusion of hot carriers is not important. We also found that the overall width of the luminescence spectrum is more sensitive to μ and hence to the electron density than to the electron temperature [the high-energy tail of the spectrum is, however, very sensitive to the electron temperature as expected from Eq. (16)]. In Fig. 10 we plot the FWHM of the luminescence spectra as a function of electron density at $T_e = 500$ K. Thus the FWHM of the luminescence spectra can serve as a direct and quick way to estimate the photoexcited electron density.

Figure 11 shows a typical Raman spectrum after subtracting the luminescence background. The shaded and relatively sharper peaks are due to scattering by the so-called coupled LO-phonon–plasmon mode. For electron densities higher than 10^{17} cm^{-3}, the plasmon frequency in GaAs becomes very close to the LO-phonon frequency.[7] As a result the two longitudinal waves are coupled via their macroscopic electric field. It is no longer possible to separate the vibration of the atoms from that of the electrons. For brevity we will refer to such coupled modes as the LO phonons in the rest of this article. As

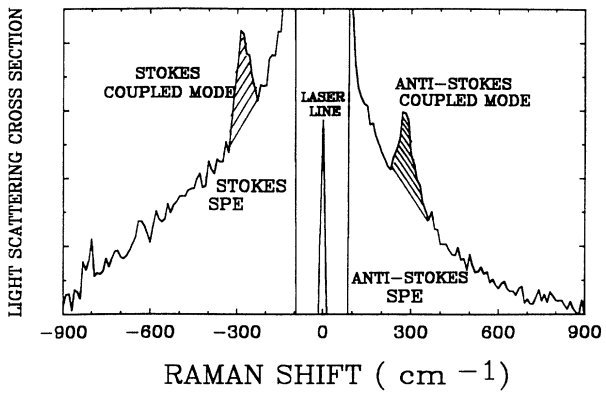

FIG. 11. Typical Raman spectrum of photoexcited hot electrons and phonons after subtracting the luminescence background. The shaded peaks represent scattering by the coupled LO-phonon–plasmon mode while the broader peak centered at the laser line is due to scattering by single-particle excitations (SPE).

pointed out in Ref. 7, when the electron density has a Gaussian spatial distribution, as in case of electrons excited by a focused laser beam, the coupled LO-plasmon modes appeared as two peaks near the TO- and LO-phonon frequencies in the Raman spectra. As the electron density is changed, the relatively intensities between the two peaks also changed. At high excitation densities the Raman spectrum is dominated by the peak at the TO-phonon frequency. Because of the shorter laser-pulse lengths and hence larger spectral width of the CPM laser used in our experiment, we were not able to resolve the two peaks. However, we found that the position of the broadened coupled-mode peak shifted towards the TO-phonon frequency as the electron density was increased. This result, shown in Fig. 12 as solid circles, suggested that in comparing the experimental results with theory we can correct for the effect of spatial inhomogeneity of

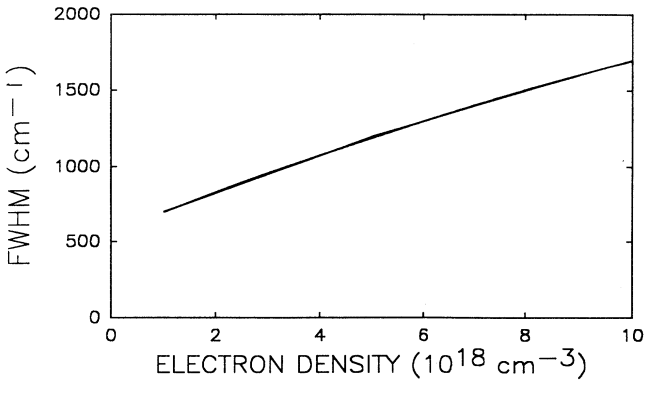

FIG. 10. FWHM of the time-integrated luminescence spectra of GaAs deduced from the theoretical curves calculated from Eq. (16) plotted against the electron density at $T = 500$ K.

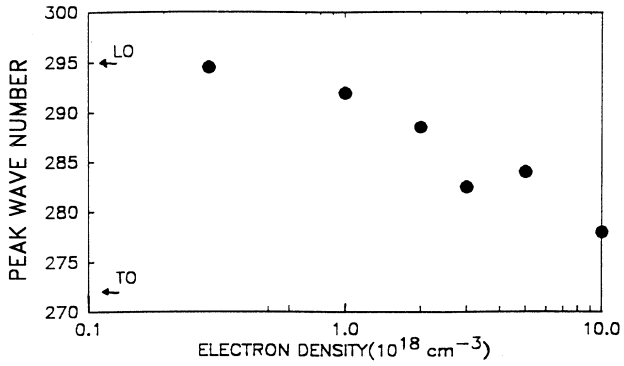

FIG. 12. Dependence of the peak position of coupled LO-phonon–plasmon mode in GaAs on photoexcited electron density obtained with CPM laser pulses with a bandwidth of 30 cm^{-1}. The two peaks at the TO- and LO-phonon frequencies cannot be resolved because of large bandwidth.

the electron gas in the same way as in Ref. 7. This correction is important only at densities below 5×10^{18} cm^{-3}. Above this density the Raman spectra are dominated by the high-density region peak at the TO-phonon frequency. The LO-phonon occupation numbers N_q are determined from the ratio of the anti-Stokes intensity I_{AS} and Stokes intensity I_S by the equation[18]

$$N_q=[(I_S/I_{AS})-1]^{-1} . \tag{17}$$

It should be noted that in determining N_q, we have to take into account possible resonance effects in the Raman cross section. Such effect can be corrected for by measuring the phonon Raman cross section with a cw tunable dye laser. The phonon temperatures calculated from N_q are plotted as a function of the total excited electron densities in Figs. 13 and 14. The solid circles are the experimental points. The results in Fig. 13 were obtained at low electron densities at 77 K while the results in Fig. 14 were taken at room temperature and at higher electron densities. At low electron density there are fewer hot phonons emitted by hot electrons so it is necessary to cool the sample to decrease the background due to thermal phonons. We note that at low densities the phonon temperature increases almost linearly with electron density, but at electron densities around 10^{18} cm^{-3} the phonon temperature starts to saturate. In Fig. 14 we find a similar trend at 300 K, except in this case much higher electron densities were obtainable by focusing the laser on the sample with a lens with shorter focal length. In this case the phonon temperature remains almost unchanged for electron densities between 2×10^{18} cm^{-3} and 8×10^{18} cm^{-3}.

We have identified the broader peak centered around the laser line in Fig. 11 as due to electronic Raman scattering caused by the photoexcited hot electrons. We base this conclusion on the fact that this peak is absent at low electron densities and it grows quadratically with electron density. Similar electronic Raman scattering peak due to photoexcited electrons has been identified

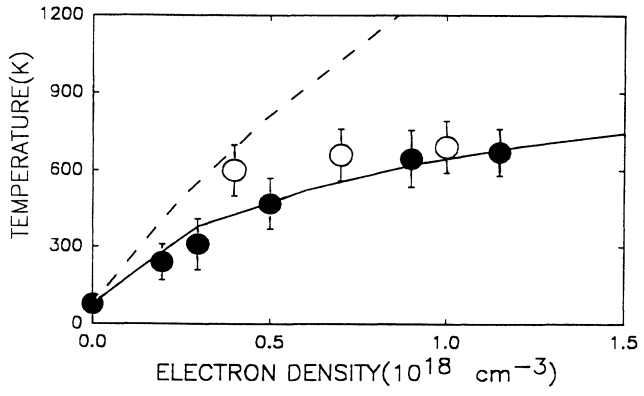

FIG. 13. T_e (open circle) and T_q (closed circle) in GaAs at 77 K excited by laser pulses of 600 fs FWHM. The solid curve is the result of the multivalley model calculation for T_q while the dashed curve is the result of the one-valley model for T_q.

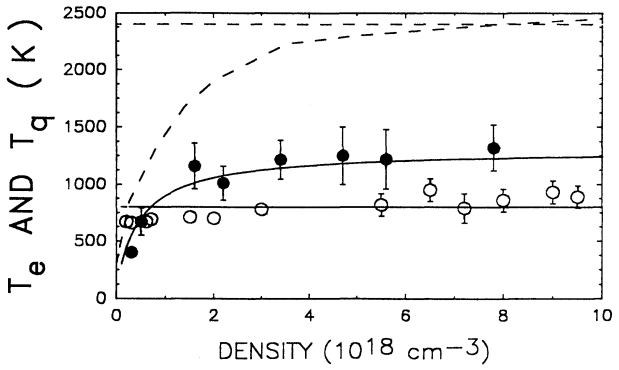

FIG. 14. Measured T_e (open circle) and T_q (closed circle) plotted as a function of the photoexcited electron density in GaAs at 300 K. The solid and dashed lines are results of fit obtained with multivalley and one-valley model calculations, respectively, using $D_{\Gamma-L}=7\times10^8$ eV/cm.

previously.[7,8] It is known that mobile electrons can scatter light via several different mechanisms.[31] In the backscattering configuration used in our experiment with the scattered radiation polarized parallel to the incident radiation, the spin-density fluctuation mechanism is forbidden.[32,33] Considering the high carrier densities achieved in our experiment, we expect that the charge-density fluctuation mechanism is also unlikely.[32] On the other hand, the high temperature of the electrons in our experiment makes energy-density fluctuations (EDF) the most likely mechanism responsible for the observed electronic Raman scattering.[34] The line shape of the electronic Raman peak we observe can be fitted by an asymmetric Lorentzian. A similar Lorentzian line shape has been observed in previous Raman scattering from free carriers in doped semiconductors[34] and from photoexcited electron plasma.[8] To determine the electron temperature we use the result that the electronic Raman cross section for SPE, σ can be expressed as[31]

$$\sigma(\mathbf{q},\omega)\propto\frac{1}{e(\hbar\omega/k_bT)-1}\mathrm{Im}K(\mathbf{q},\omega) , \tag{18}$$

where K is linear response function of the electron gas to an external electric field. Using time-reversal symmetry it can be shown that[35]

$$K(\mathbf{q},\omega)=K^*(\mathbf{q},-\omega) . \tag{19}$$

Using the above two equations we arrive at this expression:[8]

$$\exp[\hbar\omega/k_bT_e]=\sigma(\mathbf{q},-\omega)/\sigma(\mathbf{q},\omega) , \tag{20}$$

which shows that the electron temperature can be determined also from the ratio of the anti-Stokes to Stokes Raman intensities.

The electronic Raman peak is much broader than the coupled LO-phonon peaks so there is no unique choice for the Raman frequency ω in determining T_e. Since the photoexcited electrons are cooling during the duration of the laser pulse when a single beam is used to both excite

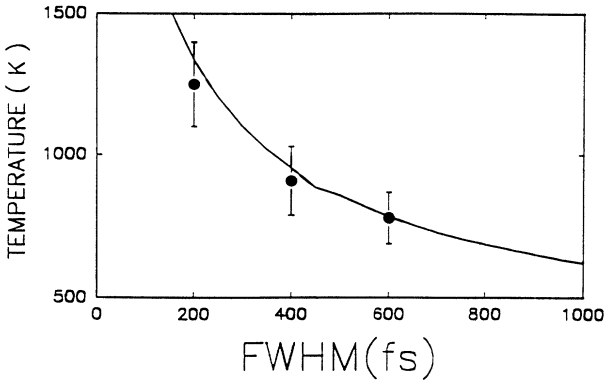

FIG. 15. Cooling curve of photoexcited hot electrons in GaAs at 300 K obtained by measuring the electron temperature as a function of the FWHM of laser pulses.

and probe the electron gas, it is possible that the electron temperature deduced from different Raman frequencies are different. For example, at short times the electrons are hotter so they produce a broader Raman spectrum. As a result, T_e determined from a larger ω may be higher than T_e determined from a smaller ω. If this is true then no well-defined electron temperature can be obtained from the Raman spectra. For subpicosecond laser pulses we find that the electron temperature determined from different values of ω is usually constant to within 10%. Furthermore, the measured temperature changes with the laser-pulse length as a result of the cooling of the electron gas.[10] Figure 15 shows the electron temperature as a function of the laser FWHM at a constant density of 3×10^{18} cm^{-3}. Using a constant pulse length of 600 fs we have determined both the electron and phonon temperatures from the same Raman spectra as a function of electron density. The results are shown in Figs. 13 and 14 as the open (electron temperature) and closed circles (phonon temperature).

V. DISCUSSIONS

The crucial results of our experiment are represented by the data points in Figs. 13–15. These results can be compared with the predictions of the one-valley model and of the multivalley model presented in Secs. II A and II B. It is easily seen that the one-valley model can explain the experimental results only *qualitatively* and not *quantitatively*. The fast cooling rate of the hot electrons in Fig. 15 and the large overshoot in T_e by T_q cannot be explained by the one-valley model. These discrepancies cannot be removed by adjusting parameters in the model calculation since all the parameters are known in the one-valley model. On the other hand, the experimental results can be explained quantitatively by the multivalley model. We will now compare in detail the experimental results with the prediction of the multivalley model.

Figure 15 shows that the electron temperature decreased from 1250 to 900 K when we increased the pulse width from 200 to 400 fs. Using the result that the electron temperature determined with a pulse FWHM of δt is equal to the temperature of the electron after cooling for an equivalent duration $0.4\delta t$ when excited by an infinitely short pulse, we estimated that the electron cooling rate is equal to $\frac{3}{2}(1250-900)k_b/(0.4\times200$ fs) or about 562 meV/ps. This crude calcualtion underestimates the actual cooling rate since it assumes that the electron cooling rate is constant and independent of temperature, whereas we expect that the cooling rate is larger at higher temperatures. However, this rate already is about three times larger than that calculated from the Fröhlich interaction *without considering the hot-phonon effect.* On the other hand, such a faster cooling rate is consistent with IVS. For example, by using $D_{\Gamma-L}=7\times10^8$ eV/cm^{-1}, we obtain the solid curve in Fig. 15. The general shape of the cooling curve agrees with the experiment. If $D_{\Gamma-L}$ is known, we can calculated the dependence of the hot-phonon population and temperature on electron density within the multivalley model presented in Sec. II B. The effect of using laser pulse with $\delta t=600$ fs is taken into account in the manner discussed in Sec. II C; namely, the electron gas is assumed to be excited by a δ-function pulse and the measured T_e is compared with the calculated T_e after cooling for a duration of $0.4\delta t$. The results are shown as solid curves in Figs. 13 and 14. They have been fitted to the experimental points by adjusting $D_{\Gamma-L}$ to equal to 7×10^8 eV/cm^{-1}. We estimate that the error in the value of $D_{\Gamma-L}$ obtained in this way is about 30%, resulting mainly from the uncertainties in the electron and phonon temperatures. For comparison, we show as the dashed curves in Figs. 13 and 14 the density dependence of the electron and phonon temperatures predicted by the one-valley model. The difference between the two models is quite clear. We note in particular that the multivalley model accounted very well for both the magnitude of the phonon temperature overshoot and also the electron density at which this overshoot occurred. Thus our results provide convincing evidence that the *cooling of the hot photoexcited carriers in bulk GaAs in subpicosecond time scale is dominated by intervalley scattering.* We also note that while the cooling rate of the hot electron is dependent upon intervalley scattering, the linear dependence of the hot LO-phonon population on the electron density in the low-density regime is determined mainly by the electron-LO-phonon interaction. Within the subpicosecond time of our experiment, LO-phonon decay is negligible. Thus one way to determine the electron–LO-phonon interaction that does not involve measuring the rise time of the LO-phonon population[13] or the electron decay time is to measure the LO-phonon population as a function of the photoexcited electron density.

As we pointed out earlier, there were large variations in the value of the deformation potential for Γ to L IVS. Values of $D_{\Gamma-L}$ quoted in the literature used to vary from 10^8 to 10^9 eV/cm.[25] More recently the range of values has narrowed down to between 3×10^8 and 8×10^8 eV/cm. The value of $D_{\Gamma-L}$ deduced in the present experiment agrees very well with the value of 6.5×10^8 eV/cm determined by Shah *et al.*[6] using subpicosecond time-resolved photoluminescence, but is about 50%

larger than the value deduced by Ulbrich *et al.*[25] from cw hot luminescence. Zollner *et al.*[36] have pointed out that this discrepancy can be explained by the different lattice temperatures in the various experiments. While the present experiment and that of Shah *et al.*[6] were performed at room temperature, the experiment of Ulbrich *et al.*[25] was carried out at 25 K. Zollner *et al.*[36] pointed out that the usual selection rules for IVS (Ref. 37) were strictly valid for electrons located at the zone center. However, in most experiments studying IVS the electrons involved typically have wave vectors of the order of 10^7 cm^{-1} because of their large kinetic energy. As a result, IVS of these electrons with emission of the zone-edge TA phonon is not strictly forbidden. Since the TA phonons have lower energy than the LA and LO phonons, scattering with the TA phonons is much more important at room temperature than at low temperature. Thus one should interpret the deformation potential determined by Ulbrich *et al.*[25] as mainly due to emission of the zone-edge LA and LO phonons. On the other hand, the deformation potential determined in the present work and in the experiment of Shah *et al.*[6] at room temperature contains contributions from all the zone-edge phonons.

Finally, we note that in Fig. 14 the electron temperature showed a slight tendency to increase with the photoexcited electron density. This trend is not expected if the electron cooling mechanism is dominated by electron-hole or electron-electron scattering. If the dominant cooling mechanism is IVS as we have concluded, the electron temperature should be independent of the electron density since the short-range deformation potentials are not screened by electron densities of 10^{19} cm^{-3} or even higher.[38] We do not have a definite explanation for this result at this time.

In conclusion we find that *inter*valley scatterings play an important role in the cooling of photoexcited hot electrons. As a result of this very rapid cooling the temperature of the hot LO phonons generated by the hot electrons temporarily overshoot the electron temperature. From the electron cooling curve and the dependence of the hot-phonon temperature on the excited electron density, we have determined the deformation potential for scattering between the Γ and L conduction-band valleys in GaAs.

ACKNOWLEDGMENTS

We are grateful to Dr. Henry Lee and Professor Shyh Wang for providing us with the MBE grown GaAs sample used in our experiment. This research was supported by the Director, Office of Energy Research, Office of Basic Energy Science, Materials Sciences Division of the U.S. Department of Energy under Contract No. DE-AC03-76SF00098.

[1]See, for example, E. M. Conwell, *Solid State Physics: Advances in Research and Applications,* edited by F. Seitz (Academic, New York, 1967), Suppl. 9.

[2]E. M. Conwell and M. O. Vassel, IEEE Trans. Electron. Devices **ED-13**, 22 (1966).

[3]W. Z. Lin, L. G. Fujimoto, E. P. Ippen, and R. A. Logan, Appl. Phys. Lett. **50**, 124 (1987).

[4]C. L. Tang, F. W. Wise, and I. A. Walmsley, Solid State Electron. **31**, 439 (1988).

[5]W. H. Knox, C. Hirlimann, D. A. B. Miller, J. Shah, D. S. Chemla, and C. V. Shank, Phys. Rev. Lett. **56**, 1191 (1986).

[6]J. Shah, B. Deveaud, T. C. Damen, W. T. Tsang, and P. Lugli, Phys. Rev. Lett. **59**, 2222 (1987).

[7]C. L. Collins, and P. Y. Yu, Solid State Commun. **51**, 123 (1984).

[8]Y. H. Huang and P. Y. Yu, Solid State Commun. **63**, 109 (1987).

[9]D. S. Kim and P. Y. Yu, Appl. Phys. Lett. **56**, 1570 (1990).

[10]D. S. Kim and P. Y. Yu, Appl. Phys. Lett. **56**, 2210 (1990).

[11]A summary of this work has appeared in D. S. Kim and P. Y. Yu, Phys. Rev. Lett. **64**, 946 (1990).

[12]R. F. Leheny, J. Shah, R. L. Fork, C. V. Shank, and A. Migus, Solid State Commun. **31**, 809 (1979).

[13]J. A. Kash, J. M. Hvam, and J. C. Tsang, Phys. Rev. Lett. **54**, 2151 (1985).

[14]P. Lugli and D. K. Ferry, Physica B **134**, 364 (1985); P. Lugli, Solid State Electron. **31**, 667 (1988); L. Rota and P. Lugli, *ibid.* **32**, 1423 (1989).

[15]D. Hulin, A. Migus, A. Antonetti, and J. L. Oudar, in *Proceedings of the 18th International Conference on the Physics of Semiconductors,* edited by O. Engstrom (World Scientific, Singapore, 1987), p. 1279.

[16]J. A. Kash and J. C. Tsang, Ref. 15, p. 1287.

[17]M. A. Osman and D. K. Ferry, Phys. Rev. B **36**, 6018 (1987).

[18]C. L. Collins and P. Y. Yu, Phys. Rev. B **30**, 4501 (1984).

[19]H. Sato and Y Hori, Phys. Rev. B **36**, 6033 (1987).

[20]See, for example, C. Kittel, *Introduction to Solid State Physics,* 6th ed. (Wiley, New York, 1986), p. 266.

[21]J. Shah, A. Pinczuk, A. C. Gossard, and W. Wiegmann, Phys. Rev. Lett. **54**, 2045 (1985).

[22]W. Potz and P. Kocevar, Phys. Rev. B **28**, 7040 (1983).

[23]W. Cai, M. C. Marchetti, and M. Lax, Phys. Rev. B **35**, 1369 (1987).

[24]W. W. Ruhle, K. Leo, and E. Bauser, Phys. Rev. B **40**, 1756 (1989).

[25]R. G. Ulbrich, J. A. Kash, and J. C. Tsang, Phys. Rev. Lett. **62**, 949 (1989).

[26]Similar results have been obtained by Monte Carlo simulation on supercomputers. See, for example, the article by K. Hess in Phys. Today **43**, 34 (1990).

[27]R. L. Fork, B. I. Greene, and C. V. Shank, Appl. Phys. Lett. **38**, 671 (1981).

[28]J. A. Valdmanis and R. L. Fork, IEEE J. Quantum Electron. **QE-22**, 112 (1986).

[29]O. E. Martinez, R. L. Fork, and J. P. Gordon, Opt. Lett. **9**, 156 (1984).

[30]Y. H. Huang, P. Y. Yu, H. Lee, and S. Wang, Appl. Phys. Lett. **52**, 579 (1988).

[31]See, for example, the article by M. V. Klein, in *Light Scattering in Solids,* Vol. 8 of *Topics in Applied Physics,* edited by M. Cardona (Springer-Verlag, New York, 1975), p. 148.

[32]A. Mooradian and A. L. McWhorter, in *Light Scattering Spec-*

tra of Solids, edited by G. Wright (Springer-Verlag, New York, 1969), p. 297.

[33]P. A. Wolff, in *Scattering Spectra of Solids,* edited by G. Wright (Springer-Verlag, New York, 1969), p. 273.

[34]B. Kh. Bairamov, V. A. Voitenko, I. P. Ipatova, A. V. Subashiev, V. V. Toporov, and E. Yane, Fiz. Tver. Tela (Leningrad) **28**, 754 (1986) [Sov. Phys.—Solid State **28**, 420 (1986)].

[35]R. Kubo, J. Phys. Soc. Jpn. **12**, 570 (1957).

[36]S. Zollner, S. Gopalan, and M. Cardona, in *Proceedings of SPIE Conference on Ultrafast Laser Probe Phenomena in Bulk and Microstructure Semiconductors III,* edited by R. R. Alfano (SPIE, Bellingham, 1990), p. 78.

[37]J. L. Birman, M. Lax, and R. Loudon, Phys. Rev. **145**, 620 (1966).

[38]E. J. Yoffa, Phys. Rev. B **23**, 1909 (1981).